

Synthesis of 2-Amido-3-hydroxypyridin-4(1*H*)-ones: Novel Iron Chelators with Enhanced $p\text{Fe}^{3+}$ Values

Zu D. Liu, S. Piyamongkol, Ding Y. Liu, Hicham H. Khodr, Shu L. Lu
and Robert C. Hider*

Department of Pharmacy, King's College London, Franklin-Wilkins Building, 150 Stamford Street, London SE1 8WA, UK

Received 27 April 2000; accepted 14 August 2000

Abstract—The synthesis of a range of 2-amido-3-hydroxypyridin-4-ones as bidentate iron(III) chelators with potential for oral administration is described. The pK_a values of the ligands together with the stability constants of their iron(III) complexes have been determined. Results indicate that the introduction of an amido substituent at the 2-position leads to an appreciable enhancement of the $p\text{Fe}^{3+}$ values. The ability of these novel 3-hydroxypyridin-4-ones to facilitate the iron excretion in bile was investigated using a ^{59}Fe -ferritin loaded rat model. The optimal effect was observed with the *N*-methyl amido derivative **15b**, which has an associated $p\text{Fe}^{3+}$ value of 21.7, more than two orders of magnitude higher than that of deferiprone (1,2-dimethyl-3-hydroxypyridin-4-one) **1a** ($p\text{Fe}^{3+} = 19.4$). Dose response studies suggest that chelators with high $p\text{Fe}^{3+}$ values scavenge iron more effectively at lower doses when compared with simple dialkyl substituted hydroxypyridinones. © 2001 Elsevier Science Ltd. All rights reserved.

Introduction

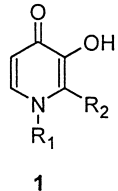
The most frequent treatment of haemoglobinopathic disorders such as β -thalassaemia major is to maintain high levels of haemoglobin by regular blood transfusion. Because man lacks a physiological means of eliminating excess iron, iron associated with transfused red cells progressively accumulates, in the liver and other highly perfused organs, leading to tissue damage, organ failure and eventually death.¹ Complications associated with elevated iron levels can be largely avoided by the use of iron-specific chelating agents and in particular desferrioxamine (DFO). Unfortunately, DFO lacks oral activity and has to be administered parenterally. This inevitably leads to poor patient compliance.² In an attempt to overcome the disadvantages associated with DFO, the successful design of an orally active, non-toxic, selective iron chelator has been a much sort after goal. In designing iron chelators for clinical application, metal selectivity and ligand-metal complex stability are

of paramount importance.^{3,4} A suitable comparator for ligands is the $p\text{Fe}^{3+}$ value, defined as the negative logarithm of the concentration of the free iron(III) in solution. Typically $p\text{Fe}^{3+}$ values are calculated for total [ligand] = 10^{-5} M, total [iron] = 10^{-6} M at pH 7.4. The comparison of ligands using this parameter is useful, since $p\text{Fe}^{3+}$, unlike the corresponding stability constants, takes into account the effects of ligand basicity, denticity and degree of protonation, as well as differences in metal–ligand stoichiometries. Chelators with high $p\text{Fe}^{3+}$ values are predicted not only to scavenge iron more effectively at low ligand concentrations, but also dissociate less readily and therefore form lower concentrations of the partially co-ordinated complexes.

3-Hydroxypyridin-4-ones (HPOs) (**1**) (Table 1) are currently one of the main candidates for the development of orally active iron chelators.³ Indeed, the 1,2-dimethyl derivative **1a** (deferiprone), with an associated $p\text{Fe}^{3+}$ value of 19.4, is the only orally active iron chelator currently available for clinical use (marketed by Apotex Inc., Toronto, Canada as FerriproxTM). In order to further improve chelation efficacy and minimise drug-induced toxicity, considerable effort has been put into the design of novel hydroxypyridinones with enhanced $p\text{Fe}^{3+}$ values.^{5,6} Novartis has produced a range of bidentate hydroxypyridinone ligands, which possess an aromatic substituent at the 2-position. The aromatic group is

Abbreviations: $p\text{Fe}^{3+}$, the negative logarithm of the concentration of the free iron(III) in solution, calculated for total [ligand] = 10^{-5} M, total [iron] = 10^{-6} M at pH 7.4; DFO, desferrioxamine; HPO, hydroxypyridinone; $D_{7.4}$, distribution coefficient at pH 7.4; MOPS, 4-morpholinepropane sulphonic acid.

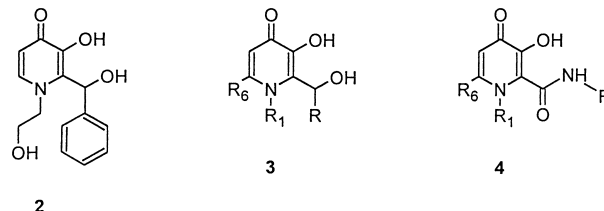
*Corresponding author. Tel.: +44-20-7848-4646; fax: +44-20-7848-4195; e-mail: robert.hider@kcl.ac.uk

Table 1. Chemical structure of selected 3-hydroxypyridin-4-ones (**1**)


Compound	R ₁	R ₂
1a (Deferiprone)	CH ₃	CH ₃
1b	CH ₂ CH ₃	CH ₂ CH ₃
1c	CH ₂ CH ₂ OH	CH ₂ CH ₃
1d	(CH ₂) ₃ OH	CH ₃

reported to stabilise the resulting iron complex and hence increase the $p\text{Fe}^{3+}$ values.⁵ The lead compound **2** was found to be orally active⁷ and highly effective at removing iron from both the iron-loaded rat and marmoset.⁵ Recently we have demonstrated that the introduction of a 1'-hydroxyalkyl group at the 2-position of 3-hydroxypyridin-4-ones **3** leads to an appreciable enhancement of $p\text{Fe}^{3+}$ values.^{6,8} This effect results from the decrease in pK_a value of the 3 and 4 pyridinone oxygens due to the combined effect of intramolecular hydrogen bonding and electron withdrawal from the pyridinone ring.⁸ Interestingly the Novartis lead compound **2** also possesses a 1'-hydroxyl group at the 2-position and this is almost certainly responsible for the observed enhanced $p\text{Fe}^{3+}$ value of the molecule. Such enhancement of $p\text{Fe}^{3+}$ values is associated with a clear improvement of chelator ability to remove iron under in vivo conditions.^{6,8} It was reasoned that the introduction of other suitable substituents, e.g., the amido function **4** at the 2-position of

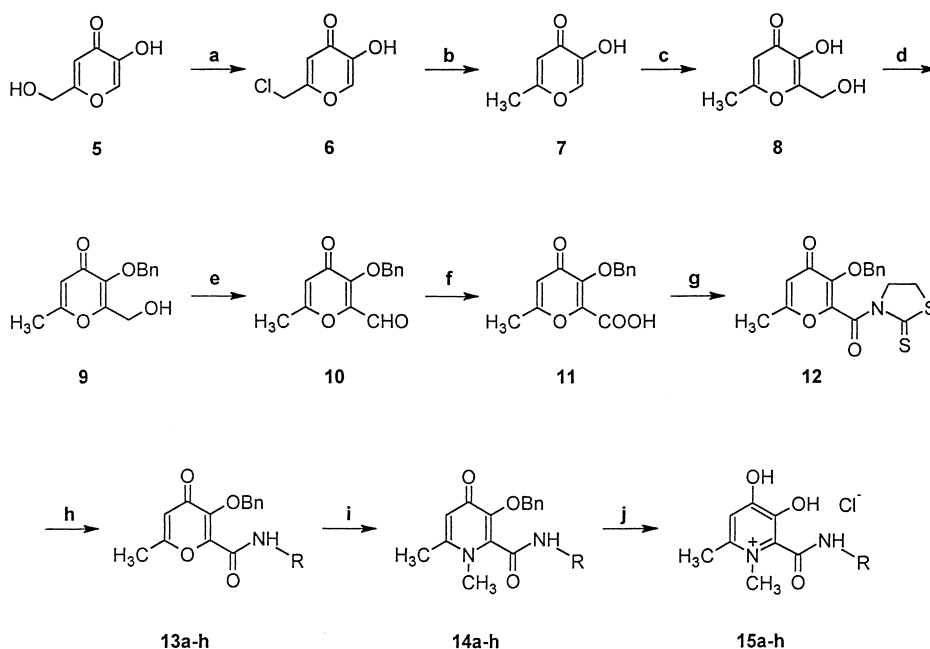
3-hydroxypyridin-4-ones would increase the $p\text{Fe}^{3+}$ value in a similar manner. A potential advantage of these 2-amido HPOs **4** is their non-chiral nature, which contrasts with the high $p\text{Fe}^{3+}$ 2-(1'-hydroxyalkyl) HPOs **2** and **3**, which possess a chiral centre. In this report, we describe the synthesis, physicochemical properties and in vivo iron mobilisation efficacies of a range of 2-amido-3-hydroxypyridin-4-ones.



Results

Chemistry

The general methodology adopted for the synthesis of 2-amido-3-hydroxypyridin-4-ones is summarised in Scheme 1. Chlorination of the 2-hydroxymethyl moiety of commercially available kojic acid **5** using neat thionyl chloride afforded 2-chloromethyl-5-hydroxypyran-4(1H)-one (chlorokojic acid) **6**, with the ring hydroxyl being unaffected. The chloro derivative **6** was subsequently reduced using zinc/hydrochloric acid to afford the 2-methyl-5-hydroxypyran-4(1H)-one **7** (58% overall yield in two steps). The α -position to the ring hydroxyl was then functionalised in an analogous fashion to the aldol condensation whereby an enolate, in this case the pyrone anion, attacks a carbonyl compound, formaldehyde, under alkaline aqueous conditions to furnish, on



Scheme 1. Synthesis of 2-amido-3-hydroxypyridin-4-ones **15a–h**. Reagents and conditions: (a) SOCl_2 , 25 °C; (b) Zn/HCl , H_2O , 65–70 °C; (c) HCHO , NaOH , H_2O , 25 °C; (d) BnBr , NaOH , $\text{CH}_3\text{OH}/\text{H}_2\text{O}$, 70 °C; (e) $\text{SO}_3 \cdot \text{pyridine}$, Et_3N , DMSO , CHCl_3 , 25 °C; (f) NaClO_2 , $\text{NH}_2\text{SO}_3\text{H}$, $\text{H}_2\text{O}/(\text{CH}_3)_2\text{CO}$, 25 °C; (g) 2-mercaptothiazoline, DCCl , DMAP , CH_2Cl_2 , 25 °C; (h) RNH_2 , CH_2Cl_2 , 25 or 40 °C; (i) CH_3NH_2 , CH_3OH , 70 °C; (j) H_2 , Pd-C , DMF , 25 °C.

acidic work up, the 2-hydroxymethylated product **8** in high yield (82%). The 3-hydroxyl group was then benzylated using benzyl bromide in good yield (80%) with no alkylation at the 2-position. The direct conversion of the primary alcohol of the protected pyranone **9** to a carboxylic acid was initially attempted by using Jones reagent. However the pyranone moiety was found to be too unstable under these conditions, producing extensive degradation. Alternatively the aldehyde was prepared before further oxidation to the carboxylic acid was attempted. The selective oxidation of the alcohol **9** to the aldehyde **10** proceeded efficiently (87.7%) by utilising sulphur trioxide pyridine complex in combination with dimethyl sulfoxide. Subsequent oxidation using sodium chlorite and sulfamic acid afforded the corresponding carboxylic acid **11** in excellent yield (85%). Activation of the carboxylic acid **11** was achieved by coupling with 2-mercaptothiazoline using dicyclohexylcarbodiimide (DCCI) as the coupling reagent and 4-dimethylaminopyridine (DMAP) as an acylation catalyst to afford the active amide **12** in 71% yield. The coupling reaction of this active amide **12** with aliphatic primary amines only required mild conditions, i.e. stirring at room temperature in an aprotic solvent such as dichloromethane, resulting with the desired 2-amido substituted pyranone analogues **13a–f** in yields generally in excess of 80%. However the analogous reaction of **12** with aromatic amines such as aniline and 3-aminopyridine under room temperature resulted in negligible reaction. Under more vigorous conditions, i.e., refluxing for a prolonged period, the required products **13g** and **13h** were isolated in moderate yields (56 and 42% respectively). Conversion of pyranone derivatives **13a–h** to the corresponding pyridinone analogues **14a–h** was then achieved by reacting with methylamine in a sealed-tube at 70 °C with methanol as solvent. The protecting benzyl group was removed by catalytic hydrogenation to yield the corresponding bidentate chelators, which were finally isolated as the hydrochloride salts **15a–h** (Table 2).

Physico-chemical characterisation

In order to demonstrate the influence of 2-amido substituent on the ligand affinity, both the pK_a values of the ligands and the stability constants of their iron(III)

complexes were evaluated using an automated titration system.^{8–10} Distribution coefficients of the chelators were measured using an automated continuous flow technique.^{8–10}

Ligand pK_a values. All ligands were investigated by simultaneous spectrophotometric and potentiometric titration.^{8–10} The pH dependence of the UV spectra of **15b** (Fig. 1) is presented as an example. A clear shift in λ_{max} is observed in the full speciation spectra of ligand **15b** over pH range 1.89–11.56 (Fig. 1) which displays the pH dependence of the ligand ionization equilibrium. The optimized pK_a values obtained from non-linear least-square regression analysis are shown in Table 2. Most of the 2-amido HPOs possess two pK_a values, one corresponding to the 4-hydroxyl function and the second corresponding to the 3-hydroxyl function (Scheme 2). The only exception is **15h** which has an extra pK_a value associated the pyridine moiety. The pK_a values obtained from spectrophotometric titration are similar and comparable to those calculated from the potentiometric titration (Table 2). The introduction of an amido substituent at the 2-position results in clear reduction in the pK_a values of both hydroxyl groups, as compared with simple dialkyl substituted HPOs such as **1a** and **1b** (Table 2).

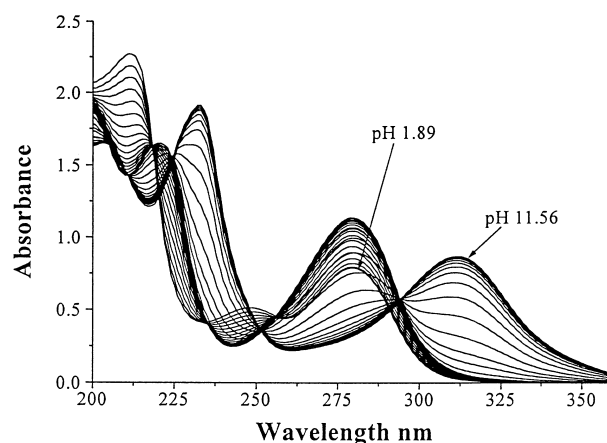


Figure 1. pH dependence of the UV spectrum of **15b** over the pH range 1.89–11.56.

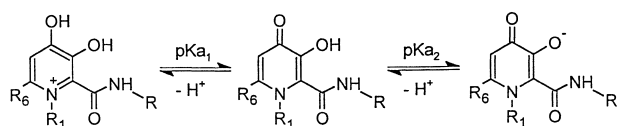
Table 2. 2-Amido-3-hydroxypyridin-4-one hydrochlorides (**15a–h**) and their measured physicochemical properties

Compound	R	pK_a		Affinity constants for Fe(III)								Log P
		Potentiometric	Spectrophotometric	Log β_3 (C) ^a	Log K_1	Log K_2	Log K_3	Log β_3 (S) ^b	pFe^{3+} (at pH 7.45)	$D_{7.4}$ ($n=5$)	F_n (at pH 7.4)	
1a	—	3.68, 9.77	3.56, 9.64	36.60	14.56	12.19	9.69	36.44	19.4	0.17	0.995	−0.767
1b	—	3.81, 9.93	ND	ND	15.20	11.76	9.84	36.80	19.7	1.78	0.997	0.252
15a	H	2.70, 8.42	2.70, 8.34	33.20	12.59	11.30	9.32	33.21	20.9	0.02 ± 0.01	0.905	−1.656
15b	CH ₃	2.75, 8.47	2.77, 8.44	34.01	13.41	11.47	9.43	34.31	21.7	0.04 ± 0.01	0.919	−1.361
15c	CH(CH ₃) ₂	2.79, 8.70	2.69, 8.61	33.66	13.10	11.38	9.24	33.72	20.7	0.30 ± 0.06	0.947	−0.499
15d	CH ₂ CH ₂ OCH ₃	2.81, 8.47	2.68, 8.44	33.61	12.68	11.49	9.38	33.55	20.9	0.04 ± 0.02	0.919	−1.361
15e	CH ₂ CH ₂ OH	2.74, 8.37	2.67, 8.27	33.33	12.85	11.18	9.30	33.33	21.2	0.02 ± 0.01	0.893	−1.650
15f	CH ₂ C ₆ H ₅	2.71, 8.45	2.62, 8.34		Not determined					13.5 ± 1.56	0.908	1.172
15g	C ₆ H ₅	2.65, 8.14	2.55, 8.10		Not determined					4.16 ± 0.90	0.840	0.695
15h	<i>m</i> -C ₃ H ₄ N	2.29, 3.92, 8.06	2.25, 3.90, 7.94	32.88	12.38	10.97	9.53	32.88	21.6	0.47 ± 0.07	0.799	−0.230

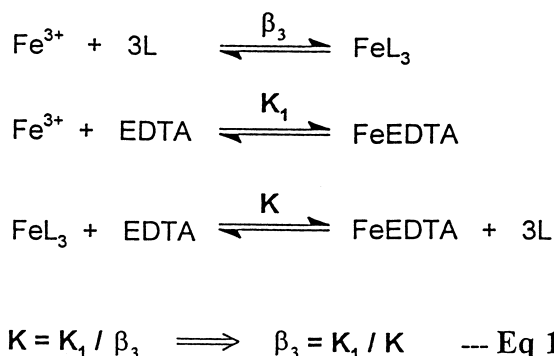
^aThe cumulative stability constants (β_3) directly measured from competitive titration with EDTA.

^bThe cumulative stability constant obtained by summation of the three stepwise equilibrium constants (K_1 , K_2 and K_3).

Stability constants of iron(III) complexes. The stability constant of an iron-ligand complex is one of the key parameters related to the *in vivo* chelation efficacy of a ligand. The cumulative stability constants (β_3) of ligands were determined spectrophotometrically by competition with the well characterised hexadentate polyamino-carboxylate ligand EDTA under defined conditions (Scheme 3).¹⁰ The resulting UV/visible spectra of ligand **15b**-iron(III) complex in competition with EDTA are shown in Figure 2. Clearly the λ_{\max} of the spectra does not shift appreciably whereas the absorbance decreases upon addition of EDTA (Fig. 2). The equilibrium constant K (Scheme 3) was determined for each EDTA addition, then by employing the literature stability constant (K_1) of EDTA, the cumulative stability constants (β_3) can be calculated from eq (1) (Scheme 3). Due to the extremely poor water solubility of the resulting iron(III) complex of ligands **15f** and **15g**, the determination of stability constants for both ligands was not attempted.



Scheme 2. Protonation equilibria of 2-amido-3-hydroxypyridin-4-ones.



Scheme 3. Competition equilibria between a bidentate ligand and EDTA for iron(III).

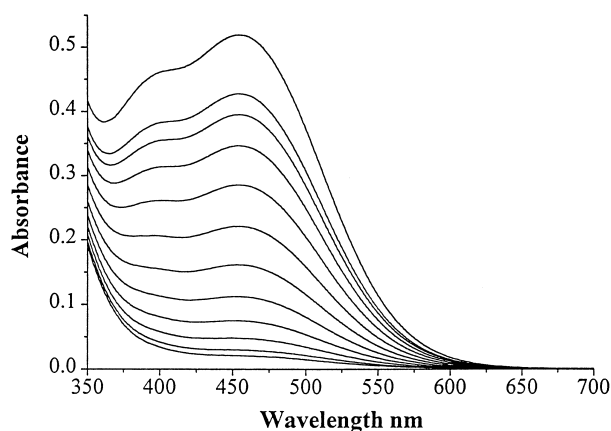
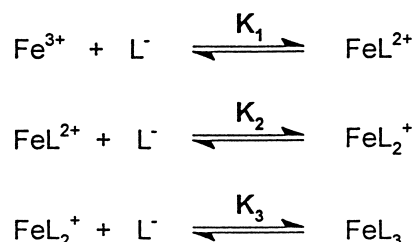


Figure 2. Visible spectra of a **15b**-iron(III) complex solution in competition with EDTA at pH 7.4. The ratio of **15b** to iron(III) was 10:1 and the iron(III) to EDTA ratio was varied from 1:0 to 1:40.

Bidentate ligands form a number of complexes with iron(III) so that aqueous solutions equilibrate to give a mixture of species, the composition of which depends on the metal ion, ligand and hydrogen ion concentrations (Scheme 4). In this current work, the stepwise equilibrium constants (K_1 , K_2 and K_3) of these bidentate ligands were evaluated using an automated spectrophotometric titration system.^{8–10} The pH titration curve for ligand **15b** in the presence of iron(III) is presented in Figure 3. A clear shift in λ_{\max} is observed in the full speciation spectra of ligand **15b**: iron(III) complexes over pH range 1.37–4.26 (Fig. 3) which displays the pH dependence of the different metal/ligand equilibrium. The optimised values are presented in Table 2, where an excellent agreement has been observed between the summation of the $\log K_1$, K_2 and K_3 and the $\log \beta_3$ value directly determined by competitive titration with EDTA (Table 2). The introduction of an amido substituent at the 2-position leads to a reduction in both $\log K$ values and $\log \beta_3$ values, as compared with simple dialkyl substituted HPOs (Table 2). Thus the $\log \beta_3$ values for 2-amido HPOs fall within the range of 32.9–34.3, as compared to 36.4 for **1a** and 36.8 for **1b**.

Distribution coefficients. The distribution coefficients ($D_{7.4}$) of the ligands between 1-octanol and MOPS buffer (pH 7.4) were determined using an automated filter-probe system.^{8–10} Since the introduction of an amido substituent significantly reduces the pK_a values of the 3-hydroxyl group (pK_{a_2}) to the range 8.0–8.6 (Table 2), the degree of ionization of this functional group at pH



Scheme 4. Complex formation of iron(III) with bidentate 3-hydroxypyridin-4-ones.

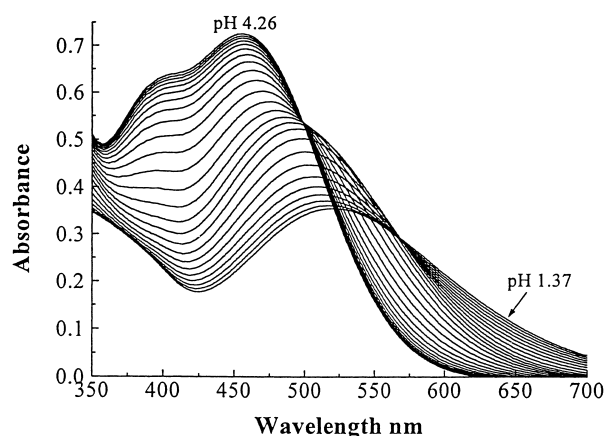


Figure 3. pH dependence of the visible absorption spectrum of ligand **15b** in the presence of iron(III) over the pH range 1.37–4.26. [iron(III)] = 1.98×10^{-4} M and [ligand **15b**] = 9.91×10^{-4} M.

7.4 becomes appreciable. As a result of the degree of ionization of the 4-hydroxyl function (pK_{a1}) being relatively small at pH 7.4, the neutral fraction (F_n) of the 2-amido HPOs can then be calculated from eq 2 by employing the pK_{a2} values determined above. Hence the partition coefficient (P) of each compound can be calculated from eq 3. The distribution coefficient values of the 2-amido HPOs cover the range 0.02–4.16 (Table 2). The aromatic derivatives **15f**, **15g** and **15h** were found to be more hydrophobic than the aliphatic analogues. Consequently, these aromatic derivatives would be expected to have better oral absorption and experience more efficient extraction by the liver, which is the major iron storage organ.

$$\text{Neutral fraction } (F_n) = \frac{1}{1 + 10^{pH - pK_{a2}}} \quad (2)$$

$$P = \frac{D_{7.4}}{F_n} = D_{7.4} \times (1 + 10^{pH - pK_{a2}}) \quad (3)$$

Iron mobilisation efficacy

In vivo iron scavenging ability of the 2-amido HPOs were compared with simple dialkyl substituted HPOs in the ^{59}Fe -ferritin labelled rat model.¹¹ Most of the aliphatic amido derivatives were found to be superior to **1a** in this model (Table 3). Surprisingly all three aromatic derivatives **15f**, **15g** and **15h**, despite their favourable lipophilicity, were found to be relatively poor iron scavengers under in vivo conditions, with efficacies of 7.5, 5.4 and 10.4%, respectively. The most effective compound was unexpectedly found to be **15b** ($D_{7.4} = 0.04$), with an associated efficacy at 450 $\mu\text{mol/kg}$ of 54.8%, being equally effective as **1b** (Table 3). Detailed dose response studies of **15b** at three different doses (150, 300 and 450 $\mu\text{mol/kg}$) further highlights its superior

performance at low doses, as compared with **1a** and **1b** (Table 3). **1b** is marginally more effective than **15b** at a dose of 450 $\mu\text{mol/kg}$, however it is markedly inferior at the dose of 150 $\mu\text{mol/kg}$. Indeed, **15b** was found to be more effective at 150 $\mu\text{mol/kg}$ than **1a** (Deferiprone) at 450 $\mu\text{mol/kg}$ (Table 3).

In vivo metabolism

In order to understand the potential influence of the in vivo biotransformation of these 2-amido substituted hydroxypyridinones on their iron scavenging efficacy, the metabolism of two selected 2-amido HPOs (**15b** and **15h**) has been investigated in the rat. Bile cannulation studies demonstrate that the amount of excreted unchanged pyridinone is markedly different for the two chelators (Table 4). With **15b** there is very little formation of a glucuronide, which is in contrast to **15h**, where over 50% of the oral dose is excreted as the 3-*O*-glucuronide metabolite (Table 4). There is a high level of unchanged **15b** present in the urine, whereas the phase II glucuronide conjugate is the major excreted species for **15h** (Table 4).

Discussion

In order to further optimise the physicochemical properties, in particular the $p\text{Fe}^{3+}$ values of 3-hydroxypyridin-4-ones iron chelators, a range of 2-amido HPOs have been synthesised and subjected to physicochemical analysis. It is clear that, like the 2-(1'-hydroxyalkyl) derivatives, the introduction of an amide function at the 2-position of 3-hydroxypyridin-4-ones leads to a reduction of the pK_a values (Table 2). This effect results from stabilising the ionised species due to the combined effect of the negative inductive effect of the 2-amido group from the pyridinone ring and possible intramolecular hydrogen bonding between the 2-amido group and the adjacent 3-hydroxyl function **16**. Although such an effect reduces the overall stability constants for iron(III) (Table 2), it also reduces the affinity of the chelating function for protons. These changes result in an increase in the corresponding $p\text{Fe}^{3+}$ values at pH 7.4, where the values fall in the range 20.7–21.7 as compared to that of **1a** (deferiprone), namely 19.4. A similar reduction on pK_a values and hence enhancement on the $p\text{Fe}^{3+}$ values

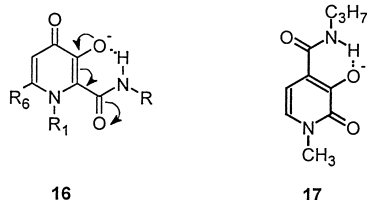
Table 3. Iron mobilisation efficacy studies of 2-amido-3-hydroxypyridin-4-ones (**15a–h**) in the ^{59}Fe -ferritin loaded rat model. All chelators were given orally and control rats were administered with an equivalent volume of water. Values are expressed as means \pm SD ($n = 5$)

Chelator	Dose ($\mu\text{mol/kg}$)	Iron mobilisation (%)	Efficacy (%)
Control	—	3.87 \pm 1.0	0.0
1a	450	13.4 \pm 5.2	9.5
1a	300	9.2 \pm 2.2	5.4
1a	150	6.3 \pm 2.1	2.4
1b	450	59.7 \pm 10.9	55.8
1b	300	35.7 \pm 4.4	31.8
1b	150	16.5 \pm 6.2	12.6
1c	450	16.8 \pm 2.7	12.9
1d	450	29.9 \pm 3.8	26.0
15a	450	10.1 \pm 3.7	6.2
15b	450	58.7 \pm 7.8	54.8
15b	300	54.1 \pm 14.1	50.2
15b	150	33.1 \pm 6.8	29.2
15c	450	45.8 \pm 6.1	41.9
15d	450	40.9 \pm 7.1	37.0
15e	450	29.2 \pm 6.3	25.3
15f	450	11.4 \pm 1.8	7.5
15g	450	9.28 \pm 2.8	5.4
15h	450	14.3 \pm 2.8	10.4

Table 4. Amount of unchanged chelators and their glucuronidated metabolites found in bile, urine and faeces and gut contents after oral administration of **15b** or **15h**. Values are expressed as mean \pm SD. The values in brackets are the percentage of the given dose (450 $\mu\text{mol/kg}$, or 94.5 μmol /each rat)

		15b ($n = 3$) (μmol)	15h ($n = 4$) (μmol)
In bile	Unchanged chelator	6.4 \pm 0.8 (6.8%)	1.6 \pm 0.5 (1.7%)
	Glucuronide	6.0 \pm 0.9 (6.4%)	50.2 \pm 12.0 (53.1%)
In urine	Unchanged chelator	18.7 \pm 2.6 (20.0%)	1.1 \pm 0.4 (1.2%)
	Glucuronide	14.5 \pm 1.9 (15.3%)	11.2 \pm 5.2 (11.9%)
In faeces and gut contents	Unchanged chelator	5.5 \pm 3.0 (5.7%)	Not detectable

has been previously observed by the introduction of an amide function at the 4-position of 3-hydroxy-pyridin-2-ones **17**.¹² The introduction of an amido substituent at the 2-position of 3-hydroxypyridin-4-ones has a dramatic effect on the speciation plot of the iron (III) complexes as presented in Figure 4. This indicates that **15b** will dissociate less readily leading to lower concentrations of the L_2Fe^{3+} complex in the pH range 5.5–7.0, as compared with **1a**.



In vivo iron mobilisation efficacy of this series of compounds has been investigated in a non-iron overloaded rat model originally developed by Pippard et al.¹³ ⁵⁹Fe-ferritin has been used to label the liver iron pool, followed by a challenge with test chelator at a time when iron released by lysosomal degradation of ferritin is maximally available.^{11,13} Since the liver is the major iron storage organ under iron-overloaded conditions, this method comes close of being an ideal animal model to assess oral bioavailability and to compare the ability of chelators to remove iron from liver. In this model, desferrioxamine (DFO), deferiprone and diethylenetriaminepentaacetic acid (DTPA) all behave in manner similar to that observed clinically.^{11,13} Furthermore this method produces highly reproducible data of the type necessary for dose–response investigations and structure–activity studies.¹³ Several high pFe^{3+} 2-amido-hydroxypyridinones such as **15b**, **15c** and **15d** lead to superior iron excretion via the bile than does deferiprone **1a** (Table 3). However not all the high pFe^{3+} ligands provide enhanced efficacy, thus **15a**, **15f**, **15g** and **15h** are poor scavengers of iron under in vivo conditions, indicating that the pFe^{3+} value is not the only factor which influences chelator efficacy. Some interesting features also emerge from the structure–activity studies, **15b** was found

to be more effective not only than the more hydrophobic analogue **15c**, but also **15d** and **15e** which have very similar $D_{7.4}$ values to that of **15b**. Furthermore, the primary amido analogue **15a** is markedly inferior to **15b**. These differences highlight structural features of **15b** which are associated with its high efficacy.

All three aromatic derivatives, **15f**, **15g** and **15h**, are markedly less efficient than **15b** in the iron scavenging studies. This may result from the unfavourable phase II metabolism associated with those aromatic derivatives (Table 4). Since the 3-hydroxyl functionality is crucial for scavenging iron, such extensive biotransformation to the non-chelating 3-*O*-glucuronide conjugate severely limits the ability of chelators to mobilise iron in vivo. In contrast the phase II metabolism is only a minor metabolic pathway for **15b** (Table 4) and the lack of glucuronidation will certainly attribute to its superior efficacy in vivo. However 1-hydroxyalkyl hydroxypyridinones, namely **1c** and **1d** (Table 1), are also not extensively metabolised via phase II reactions¹⁴ and yet their iron mobilisation efficacies are much less than that of **15b** (Table 3). Clearly the chemical nature of the ligand together with its metabolic behaviour have critical impacts on the chelation efficacy of the compound. Further dose–response experiments with **15b** confirmed that chelators with high pFe^{3+} values scavenge iron more effectively at low ligand concentrations. Detailed efficacy comparisons between the different doses indicates that the efficacy of the high pFe^{3+} chelator **15b** decreases much more slowly than that of **1a** and **1b** (Table 5). The efficacy ratios of **15b** (0.533) is much greater than those for **1a** and **1b** (0.253 and 0.226, respectively) between dose 150 and 450 $\mu\text{mol/kg}$.

In summary, the introduction of an amido at the 2-position of 3-hydroxypyridin-4-ones reduces the pK_a values and hence increases the pFe^{3+} values. However, selection of the amido substituent has a dominating influence on the overall efficacy. The most effective compound was found to be **15b** which has an associated pFe^{3+} value of 21.7 compared with 19.4 for **1a** (deferiprone). It has a low $D_{7.4}$ (0.04) and yet experiences good oral absorption and liver extraction, as demonstrated by its high efficacy in the rat model. Such low lipophilicity associated with **15b** will limit the distribution of the chelator and minimise the penetration of critical biological barriers such as blood brain barrier, which in turn is likely to reduce the toxic side effects. Meanwhile, the high level of **15b** detected in the urine (Table 4) also indicates the potential of this compound to scavenge non-transferrin bound iron in the systematic circulation.

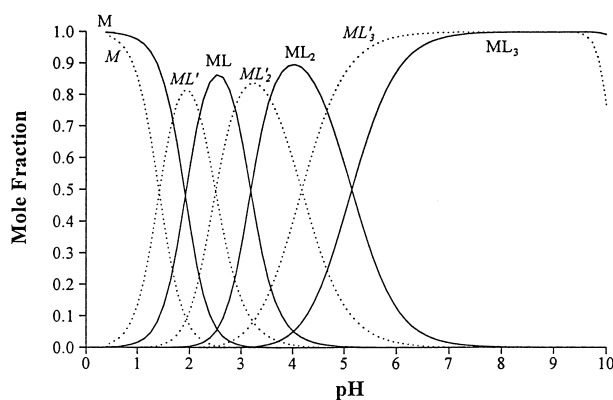


Figure 4. Comparison of the speciation plots of **1a** and **15b** in the presence of iron(III); L = **1a**; L' = **15b**; $[Fe(III)] = 1 \times 10^{-6} \text{ M}$ and $[ligand] = 1 \times 10^{-5} \text{ M}$.

Table 5. Efficacy ratio of hydroxypyridinones between different doses

Chelator	Efficacy ratio between different doses		
	$\frac{\text{Efficacy}_{(300 \mu\text{mol/kg})}}{\text{Efficacy}_{(450 \mu\text{mol/kg})}}$	$\frac{\text{Efficacy}_{(150 \mu\text{mol/kg})}}{\text{Efficacy}_{(300 \mu\text{mol/kg})}}$	$\frac{\text{Efficacy}_{(150 \mu\text{mol/kg})}}{\text{Efficacy}_{(450 \mu\text{mol/kg})}}$
1a	0.568	0.444	0.253
1b	0.570	0.396	0.226
15b	0.916	0.582	0.533

Experimental

General chemistry procedure

Melting points were determined using an Electrothermal IA 9100 Digital Melting Point Apparatus and are uncorrected. ^1H NMR spectra were recorded using a Perkin-Elmer (60 MHz) NMR spectrometer. Chemical shifts (δ) are reported in ppm downfield from the internal standard tetramethylsilane (TMS). Mass spectra (FAB) analyses were carried out by Mass Spectrometry Facility, Department of Pharmaceutical and Biological Chemistry, The School of Pharmacy, 29/39 Brunswick Square, London WC1AX, and the samples were dissolved in 3-nitrobenzyl-alcohol matrix. Elemental analyses were performed by Micro analytical laboratories, Department of Chemistry, The University of Manchester, Manchester M13 9PL.

2-Chloromethyl-5-hydroxypyran-4(1H)-one (chlorokojic acid) (6). Kojic acid **5** (50 g, 0.35 mol) was dissolved in distilled thionyl chloride (200 mL), stirred for 1 h, after which time a yellow crystalline mass formed. The product was collected by filtration and washed with petroleum ether and then recrystallised from water to give colourless needles (42.5 g, 75.9%): mp 166–168 °C (lit. value¹⁵ 166–167 °C); ^1H NMR (DMSO- d_6) δ : 4.7 (s, 2H, 6- CH_2Cl), 6.6 (s, 1H, 5-H), 8.1 (s, 1H, 2-H), 9.3 (br., s, 1H, 3-OH).

2-Methyl-5-hydroxypyran-4(1H)-one (allomaltol) (7). Chlorokojic acid **6** (30 g, 0.187 mol) was added to 100 mL of distilled water and heated to 50 °C with stirring. Zinc dust (24.4 g, 0.375 mol) was added followed by the dropwise addition of concentrated hydrochloric acid (56.1 mL) over 1 h with vigorous stirring maintaining the temperature between 70–80 °C. The reaction mixture was stirred for a further 3 h at 70 °C. The excess zinc was removed by hot filtration and the filtrate extracted with dichloromethane (3 \times 200 mL). The combined organic extracts were dried over anhydrous sodium sulphate, filtered and concentrated in vacuo to yield the crude product. Recrystallisation from isopropanol afforded colourless plates (14.8 g, 62.8%): mp 152–153 °C (lit. value¹⁵ 153–155 °C); ^1H NMR (DMSO- d_6) δ 2.25 (s, 3H, 6- CH_3), 6.2 (s, 1H, 5-H), 6.3–7.35 (br., 1H, 3-OH), 7.7 (s, 1H, 2-H).

2-Hydroxymethyl-3-hydroxy-6-methyl-pyran-4(1H)-one (8). Allomaltol **7** (12.6 g, 100 mmol) was added to an aqueous solution of sodium hydroxide (4.4 g, 110 mmol) in distilled water (100 mL) and stirred at room temperature for 5 min. 35% Formaldehyde solution (9 mL) was added dropwise over 10 min and the solution allowed stirring for 12 h. Acidification to pH 1 using concentrated hydrochloric acid and cooling to 3–5 °C for 12 h gave a crystalline deposit (12.8 g, 82%), mp 159–161 °C (lit. value¹⁵ 161–163 °C). ^1H NMR (DMSO- d_6) δ 2.3 (s, 3H, 6- CH_3), 4.5 (s, 2H, 2- CH_2OH), 4.6–5.7 (br., 1H, 2- CH_2OH), 6.25 (s, 1H, 5-H), 8.7–9.2 (br., 1H, 3-OH).

2-Hydroxymethyl-3-benzyloxy-6-methyl-pyran-4(1H)-one (9). Sodium hydroxide (4.84 g, 121 mmol, 1.1 equiv) dissolved in 10 mL distilled water was added to a solution of **8** (17.2 g, 110 mmol, 1 equiv) in methanol

(100 mL) and the reaction mixture was heated to reflux. Benzyl bromide (20.7 g, 121 mmol, 1 equiv) was added dropwise over 30 min and then refluxed for 12 h. The reaction mixture was concentrated in vacuo, the residue taken up into dichloromethane (300 mL) and the inorganic salts filtered off. The dichloromethane layer was washed with 5% sodium hydroxide solution (2 \times 100 mL), water (100 mL), dried over anhydrous sodium sulphate, filtered and concentrated in vacuo to yield the crude product as a yellow crystalline solid. Recrystallisation from dichloromethane:petroleum ether 40:60 afforded a white crystalline solid (21.6 g, 80%), mp 115–116 °C. ^1H NMR (CDCl_3) δ 2.2 (s, 3H, 6- CH_3), 2.6 (br., s, 1H, 2- CH_2OH), 4.3 (br., s, 2H, 2- CH_2OH), 5.2 (s, 2H, CH_2Ph), 6.15 (s, 1H, 5-H (pyranone)), 7.4 (s, 5H, Ar); MS (FAB): m/z , 246 [M^+]. Anal. calcd for $\text{C}_{14}\text{H}_{14}\text{O}_4$: C, 68.28; H, 5.73%. Found: C, 68.37; H, 5.66%

2-Formyl-3-benzyloxy-6-methyl-pyran-4(1H)-one (10). To a solution of **9** (5.28 g, 21.5 mmol, 1 equiv) in chloroform (100 mL) was added dimethyl sulfoxide (27 mL) and triethylamine (18.5 mL) and the reaction mixture was cooled with an ice-bath to an internal temperature of 3–5 °C. Then sulphur trioxide pyridine complex (17.1 g 107 mmol, 5 equiv) was added and the mixture was allowed to thaw to room temperature. After stirring for 12 h at room temperature, the reaction mixture was washed with water (2 \times 50 mL) and the organic phase was dried over anhydrous sodium sulphate, filtered and concentrated in vacuo to yield an orange oil. Further purification by column chromatography on silica gel (eluant: diethyl ether) furnished a white crystalline solid (4.6 g, 87.7%), mp 78–81 °C. ^1H NMR (CDCl_3) δ 2.3 (s, 3H, 6- CH_3), 5.4 (s, 2H, CH_2Ph), 6.2 (s, 1H, 5-H (pyranone)), 7.3 (s, 5H, Ar), 9.75 (s, 1H, CHO); MS (FAB): m/z , 244 [M^+]. Anal. calcd for $\text{C}_{14}\text{H}_{12}\text{O}_4$: C, 68.84; H, 4.95%. Found: C, 68.96; H, 5.07%

2-Carboxy-3-benzyloxy-6-methyl-pyran-4(1H)-one (11). To a solution of **10** (3.67 g, 15.03 mmol, 1 equiv) in acetone (50 mL)/water (50 mL) was added sulfamic acid (2.04 g, 21.04 mmol, 1.4 equiv) and 80% sodium chlorite (1.78 g, 15.8 mmol, 1.05 equiv). The reaction mixture was allowed to stir for 1 h at room temperature in an open vessel. Removal of acetone in vacuo yielded crude product as a precipitate in the remaining aqueous solution. The solid was collected, washed with absolute ethanol and dried (3.32 g, 85%), mp 173–175 °C. ^1H NMR (DMSO- d_6) δ : 2.3 (s, 3H, 6- CH_3), 5.2 (s, 2H, CH_2Ph), 6.2 (s, 1H, 5-H (pyranone)), 7.1–7.6 (m, 5H, Ar); MS (FAB): m/z , 260 [M^+]. Anal. calcd for $\text{C}_{14}\text{H}_{12}\text{O}_5$: C, 64.61; H, 4.65%. Found: C, 64.73; H, 4.89%.

N-(3-Benzyloxy-6-methyl-pyran-4(1H)-one-2-carbonyl)-1,3-thiazolidine-2-thione (12). To a vigorously stirred suspension of **11** (2.78 g, 10 mmol, 1 equiv) in dichloromethane (100 mL) was added dicyclohexylcarbodiimide (DCCI) (2.3 g, 11 mmol, 1.1 equiv) followed by the addition of 2-mercaptothiazoline (1.32 g, 11 mmol, 1.1 equiv) and a catalytic amount of 4-dimethylaminopyridine (DMAP) (50 mg). The mixture was stirred for 24 h, the white precipitate *N,N'*-dicyclohexylurea (DCU) filtered from the yellow solution and the filtrate volume

was adjusted to 200 mL with dichloromethane. The dichloromethane layer was washed with 0.1 N sodium hydroxide solution (3×100 mL), water (100 mL), dried over anhydrous sodium sulphate, filtered and concentrated in vacuo to yield the crude product as a yellow oil. Further purification by column chromatography on silica gel (eluant: ethyl acetate) furnished a bright yellow oil (2.56 g, 71%). ¹H NMR (CDCl₃) δ 2.3 (s, 3H, **6-CH₃**), 3.1 (t, 2H, **CH₂N**), 4.35 (t, 2H, **CH₂S**), 5.3 (s, 2H, **CH₂Ph**), 6.25 (s, 1H, **5-H**(pyranone)), 7.3 (s, 5H, **Ar**); MS (FAB): *m/z* 361 [*M*⁺]. Anal. calcd for C₁₇H₁₅NO₄S₂: C, 56.49; H, 4.18; N, 3.88; S, 17.74%. Found: C, 56.76; H, 4.32; N, 4.12; S, 17.86%

General procedure for the preparation of (13a–h). To a solution of **12** (3.61 g, 10 mmol, 1 equiv) in dichloromethane (100 mL) was added the corresponding primary amine (20 mmol, 2 equiv.) and the reaction mixture allowed to stir or reflux for 2–24 h. The dichloromethane layer was washed with 0.1 N sodium hydroxide solution (3×50 mL), water (50 mL), dried over anhydrous sodium sulphate, and the solvent removed in vacuo. The crude product was further purified either by recrystallization or column chromatography.

3-Benzoyloxy-6-methyl-pyran-4(1H)-one-2-carboxamide (13a). Recrystallisation from methanol/diethyl ether afforded a white crystalline solid (yield 83%), mp 157–160 °C. ¹H NMR (CDCl₃) δ 2.3 (s, 3H, **6-CH₃**), 5.3 (s, 2H, **CH₂Ph**), 6.2 (s, 1H, **5-H** (pyranone)), 7.3 (s, 5H, **Ar**); MS (FAB): *m/z* 259 [*M*⁺].

3-Benzoyloxy-6-methyl-pyran-4(1H)-one-2-carboxy-(N-methyl)-amide (13b). Recrystallisation from chloroform/petroleum ether 40–60 °C afforded a white crystalline solid (yield 88%), mp 75–78 °C. ¹H NMR (CDCl₃) δ 2.3 (s, 3H, **6-CH₃**), 2.7 (d, 3H, **CH₃NH**, *J*=6.0 Hz), 5.3 (s, 2H, **CH₂Ph**), 6.25 (s, 1H, **5-H** (pyranone)), 7.3 (s, 5H, **Ar**); MS (FAB): *m/z* 273 [*M*⁺].

3-Benzoyloxy-6-methyl-pyran-4(1H)-one-2-carboxy-(N-isopropyl)-amide (13c). Purification by column chromatography on silica gel (eluant: ethyl acetate) furnished a light yellow oil (yield 91%). ¹H NMR (CDCl₃) δ 1.0 (d, 6H, **CH(CH₃)₂**, *J*=7.0 Hz), 2.4 (s, 3H, **6-CH₃**), 3.7–4.5 (m, 1H, **CHNH**), 5.4 (s, 2H, **CH₂Ph**), 6.25 (s, 1H, **5-H**(pyranone)), 7.4 (s, 5H, **Ar**); MS (FAB): *m/z* 301 [*M*⁺].

3-Benzoyloxy-6-methyl-pyran-4(1H)-one-2-carboxy-(N-2'-methoxyethyl)-amide(13d). Purification by column chromatography on silica gel (eluant: ethyl acetate) furnished a light yellow oil (yield 94%). ¹H NMR (CDCl₃) δ 2.25 (s, 3H, **6-CH₃**), 3.2 (s, 3H, **OCH₃**), 3.0–3.6 (m, 4H, **CH₂CH₂**), 5.3 (s, 2H, **CH₂Ph**), 6.1 (s, 1H, **5-H** (pyranone)), 7.25 (s, 5H, **Ar**), 7.5–8.2 (br., 1H, **NH**); MS (FAB): *m/z* 317 [*M*⁺].

3-Benzoyloxy-6-methyl-pyran-4(1H)-one-2-carboxy-(N-2'-hydroxyethyl)-amide (13e). Purification by column chromatography on silica gel (eluant: ethyl acetate) furnished a light yellow oil (yield 90%). ¹H NMR (CDCl₃) δ 2.3 (s, 3H, **6-CH₃**), 3.1–3.8 (m, 4H, **CH₂CH₂**), 5.3 (s, 2H,

CH₂Ph), 6.15 (s, 1H, **5-H** (pyranone)), 7.3 (s, 5H, **Ar**), 7.5–8.2 (br., 1H, **NH**); MS (FAB): *m/z* 303 [*M*⁺].

3-Benzoyloxy-6-methyl-pyran-4(1H)-one-2-carboxy-(N-benzyl)-amide (13f). Recrystallisation from chloroform/petroleum ether 40–60 °C afforded a white crystalline solid (yield 86%), mp 87.5–90 °C. ¹H NMR (CDCl₃) δ 2.4 (s, 3H, **6-CH₃**), 4.4 (d, 2H, **NHCH₂Ph**, *J*=6.0 Hz), 5.3 (s, 2H, **CH₂Ph**), 6.2 (s, 1H, **5-H** (pyranone)), 7.0–7.6 (m, 10H, **Ar**), 7.8–8.3 (br., 1H, **NH**); MS (FAB): *m/z* 349 [*M*⁺].

3-Benzoyloxy-6-methyl-pyran-4(1H)-one-2-carboxy-(N-phenyl)-amide (13g). Recrystallisation from chloroform/petroleum ether 40–60 °C afforded a white crystalline solid (yield 56%), mp 132–135 °C. ¹H NMR (CDCl₃) δ 2.45 (s, 3H, **6-CH₃**), 5.5 (s, 2H, **CH₂Ph**), 6.3 (s, 1H, **5-H** (pyranone)), 7.0–7.7 (m, 10H, **Ar**), 9.4–9.9 (br., 1H, **NH**); MS (FAB): *m/z* 335 [*M*⁺].

3-Benzoyloxy-6-methyl-pyran-4(1H)-one-2-carboxy-(N-3'-pyridyl)-amide (13h). Recrystallisation from chloroform/petroleum ether 40–60 °C afforded a yellow crystalline solid (yield 42%), mp 144 °C dec. ¹H NMR (CDCl₃) δ 2.3 (s, 3H, **6-CH₃**), 5.4 (s, 2H, **CH₂Ph**), 6.2 (s, 1H, **5-H** (pyranone)), 6.8–7.4 (m, 6H, **Ar** and **5-H** (pyridine)), 7.6–8.3 (m, 3H, **2,4,6-H** (pyridine)), 9.4–9.8 (br., 1H, **NH**); MS (FAB): *m/z* 336 [*M*⁺].

General procedure for the preparation of 14a–h. To solutions of **13a–h** (5 mmol, 1 equiv) in methanol (10 mL) were added 20 mL (40 mmol, 8 equiv) of 2 M methylamine in methanol. The reaction mixtures were sealed in a thick-walled glass tube and stirred at 70 °C for 12 h. After removal of the solvent, the residues were purified either by column chromatography or recrystallization.

1,6-Dimethyl-3-benzoyloxy-pyridin-4(1H)-one-2-carboxy-amide (14a). Purification by column chromatography on silica gel (eluant: methanol:chloroform; 15:85 v/v) followed by recrystallisation from methanol/diethyl ether afforded a white crystalline solid (yield 67%), mp 210–213 °C. ¹H NMR (CDCl₃) δ 2.3 (s, 3H, **6-CH₃**), 3.45 (s, 3H, **N-CH₃**), 5.0 (s, 2H, **CH₂Ph**), 6.1 (s, 1H, **5-H** (pyridinone)), 7.3 (s, br., 5H, **Ar**), 7.8–8.4 (br, 2H, **NH₂**); MS (FAB): *m/z* 272 [*M*⁺].

1,6-Dimethyl-3-benzoyloxy-pyridin-4(1H)-one-2-carboxy-(N-methyl)-amide (14b). Recrystallisation from methanol/diethyl ether afforded a white crystalline solid (yield 82%), mp 164–165.5 °C. ¹H NMR (CDCl₃) δ 2.2 (s, 3H, **6-CH₃**), 2.65 (d, 3H, **CH₃NH**, *J*=6.0 Hz), 3.5 (s, 3H, **N-CH₃**), 4.9 (s, 2H, **CH₂Ph**), 5.95 (s, 1H, **5-H** (pyridinone)), 7.3 (s, 5H, **Ar**), 7.9–8.4 (br, 1H, **NH**); MS (FAB): *m/z* 286 [*M*⁺].

1,6-Dimethyl-3-benzoyloxy-pyridin-4(1H)-one-2-carboxy-(N-isopropyl)-amide (14c). Purification by column chromatography on silica gel (eluant: methanol:chloroform; 10:90 v/v) followed by recrystallisation from methanol/diethyl ether afforded a white crystalline solid (yield 79%), mp 176–178 °C. ¹H NMR (CDCl₃) δ 1.2 (d, 6H, **CH(CH₃)₂**, *J*=7.0 Hz), 2.1 (s, 3H, **6-CH₃**), 3.5 (s, 3H,

N-CH₃), 3.9–4.5 (m, 1H, CHN), 5.0 (s, 2H, CH₂Ph), 6.0 (s, 1H, 5-H (pyridinone)), 7.2 (s, 5H, Ar), 8.0–8.4 (br, 1H, NH); MS(FAB): *m/z* 314 [M⁺].

1,6-Dimethyl-3-benzyloxy-pyridin-4(1H)-one-2-carboxy-(N-2'-methoxyethyl)-amide (14d). Purification by column chromatography on silica gel (eluant: methanol:chloroform; 10:90 v/v) followed by recrystallisation from methanol/diethyl ether afforded a white crystalline solid (yield 82%), mp 125–126 °C. ¹H NMR (CDCl₃) δ 2.1 (s, 3H, 6-CH₃), 3.2 (s, 3H, OCH₃), 3.1–3.7 (m, 4H, CH₂CH₂), 3.4 (s, 3H, N-CH₃), 4.95 (s, 2H, CH₂Ph), 6.0 (s, 1H, 5-H (pyridinone)), 7.0–7.5 (m, 5H, Ar), 7.8–8.4 (br, 1H, NH); MS (FAB): *m/z* 330 [M⁺].

1,6-Dimethyl-3-benzyloxy-pyridin-4(1H)-one-2-carboxy-(N-2'-hydroxyethyl)-amide (14e). Purification by column chromatography on silica gel (eluant: methanol:chloroform; 15:85 v/v) followed by recrystallisation from methanol/diethyl ether afforded a white crystalline solid (yield, 86%), mp 153–155 °C. ¹H NMR (CDCl₃) δ 2.1 (s, 3H, 6-CH₃), 3.1–3.7 (m, 4H, CH₂CH₂), 3.4 (s, 3H, N-CH₃), 4.95 (s, 2H, CH₂Ph), 6.02 (s, 1H, 5-H (pyridinone)), 7.0–7.5 (m, 5H, Ar), 7.8–8.4 (br, 1H, NH); MS (FAB): *m/z* 316 [M⁺].

1,6-Dimethyl-3-benzyloxy-pyridin-4(1H)-one-2-carboxy-(N-benzyl)-amide (14f). Purification by column chromatography on silica gel (eluant: methanol:chloroform; 12:88 v/v) followed by recrystallisation from methanol/diethyl ether afforded a white crystalline solid (yield, 80%), mp 203–206 °C. ¹H NMR (CDCl₃) δ 1.9 (s, 3H, 6-CH₃), 3.4 (s, 3H, N-CH₃), 4.4 (d, 2H, NHCH₂Ph, *J* = 6.0 Hz), 4.8 (s, 2H, CH₂Ph), 5.6 (s, 1H, 5-H (pyridinone)), 7.0–7.5 (m, 10H, Ar), 8.7–9.2 (br., 1H, NH); MS (FAB): *m/z* 362 [M⁺].

1,6-Dimethyl-3-benzyloxy-pyridin-4(1H)-one-2-carboxy-(N-phenyl)-amide (14g). Recrystallisation from methanol/diethyl ether afforded a white crystalline solid (yield 92%), mp 132–135 °C. ¹H NMR (DMSO-*d*₆) δ 2.2 (s, 3H, 6-CH₃), 3.4 (s, 3H, N-CH₃), 4.95 (s, 2H, CH₂Ph), 6.1 (s, 1H, 5-H (pyridinone)), 6.8–7.7 (m, 10H, Ar); MS (FAB): *m/z* 348 [M⁺].

1,6-Dimethyl-3-benzyloxy-pyridin-4(1H)-one-2-carboxy-(N-3'-pyridyl)-amide (14h). Recrystallisation from methanol/diethyl ether afforded a yellow crystalline solid (yield 78%), mp 200 °C dec. ¹H NMR (DMSO-*d*₆) δ 2.2 (s, 3H, 6-CH₃), 3.4 (s, 3H, N-CH₃), 5.0 (s, 2H, CH₂Ph), 6.1 (s, 1H, 5-H (pyridinone)), 6.9–7.4 (m, 6H, Ar & 5-H (pyridine)), 7.8–8.7 (m, 3H, 2,4,6-H (pyridine)); MS (FAB): *m/z* 349 [M⁺].

General procedure for the preparation of 15a–h. Solutions of 14a–h in *N,N*-dimethylformamide (DMF) were subjected to hydrogenolysis in presence of 5% Pd/C (5–10% w/w of the compound) catalyst for 3 h. The catalysts were removed by filtration and the filtrates were acidified to pH 1 with concentrated hydrochloric acid. After removal of the solvents in vacuo, the residues were purified by recrystallization from methanol/diethyl ether.

1,6-Dimethyl-3-hydroxypyridin-4(1H)-one-2-carboxy-amide hydrochloride (15a). Yield 92%, mp 250 °C (dec.). ¹H NMR (DMSO-*d*₆) δ 2.4 (s, 3H, 6-CH₃), 3.65 (s, 3H, N-CH₃), 4.7–5.7 (br., OH), 7.1 (s, 1H, 5-H (pyridinone)), 8.0–8.5 (br, 2H, NH₂); MS (FAB): *m/z* 183 [(M-Cl)⁺]. Anal. calcd for C₈H₁₁ClN₂O₃: C, 43.95; H, 5.07; N, 12.81; Cl, 16.22%. Found: C, 44.23; H, 5.21; N, 12.97; Cl, 16.43%.

1,6-Dimethyl-3-hydroxypyridin-4(1H)-one-2-carboxy-(N-methyl)-amide hydrochloride (15b). Yield 93%, mp 239–240 °C. ¹H NMR (DMSO-*d*₆) δ 2.5 (s, 3H, 6-CH₃), 2.75 (d, 3H, CH₃NH, *J* = 6.0 Hz), 3.7 (s, 3H, N-CH₃), 7.2 (s, 1H, 5-H (pyridinone)), 6.8–8.1 (br, OH), 8.7–9.2 (br, 1H, NH); MS (FAB): *m/z* 197 [(M-Cl)⁺]. Anal. calcd for C₉H₁₃ClN₂O₃: C, 46.46; H, 5.63; N, 12.04; Cl, 15.24%. Found: C, 46.31; H, 5.76; N, 11.85; Cl, 15.13%.

1,6-Dimethyl-3-hydroxypyridin-4(1H)-one-2-carboxy-(N-isopropyl)-amide hydrochloride (15c). Yield 93%, mp 219–220 °C. ¹H NMR (DMSO-*d*₆) δ 1.15 (d, 6H, CH (CH₃)₂, *J* = 6.0 Hz), 2.5 (s, 3H, 6-CH₃), 3.7 (s, 3H, N-CH₃), 3.6–4.4 (m, 1H, CHNH), 5.2–6.5 (br, OH), 7.3 (s, 1H, 5-H (pyridinone)), 8.8–9.2 (br, 1H, NH); MS (FAB): *m/z* 225 [(M-Cl)⁺]. Anal. calcd for C₁₁H₁₇ClN₂O₃: C, 50.67; H, 6.57; N, 10.74; Cl, 13.60%. Found: C, 50.38; H, 6.81; N, 10.56; Cl, 13.87%.

1,6-Dimethyl-3-hydroxypyridin-4(1H)-one-2-carboxy-(N-2'-methoxyethyl)-amide hydrochloride (15d). Yield 90%, mp 204–206 °C. ¹H NMR (DMSO-*d*₆) δ 2.6 (s, 3H, 6-CH₃), 3.4 (s, 3H, OCH₃), 3.1–3.6 (m, 4H, CH₂CH₂), 3.8 (s, 3H, N-CH₃), 7.35 (s, 1H, 5-H (pyridinone)), 8.8–10.05 (br, OH and NH); MS (FAB): *m/z* 241 [(M-Cl)⁺]. Anal. calcd for C₁₁H₁₇ClN₂O₄: C, 47.74; H, 6.19; N, 10.12; Cl, 12.81%. Found: C, 47.56; H, 6.30; N, 10.36; Cl, 13.04%.

1,6-Dimethyl-3-hydroxypyridin-4(1H)-one-2-carboxy-(N-2'-hydroxyethyl)-amide hydrochloride (15e). Yield 91%, mp 178–181 °C. ¹H NMR (DMSO-*d*₆) δ 2.55 (s, 3H, 6-CH₃), 3.1–3.7 (m, 4H, CH₂CH₂), 3.85 (s, 3H, N-CH₃), 7.25 (s, 1H, 5-H (pyridinone)), 6.7–8.2 (br., OH), 9.1 (br., 1H, NH); MS (FAB): *m/z* 227 [(M-Cl)⁺]. Anal. calcd for C₁₀H₁₅ClN₂O₄: C, 45.72; H, 5.76; N, 10.66; Cl, 13.50%. Found: C, 45.47; H, 5.98; N, 10.48; Cl, 13.27%.

1,6-Dimethyl-3-hydroxypyridin-4(1H)-one-2-carboxy-(N-benzyl)-amide hydrochloride (15f). Yield 87%, mp 180–183 °C. ¹H NMR (DMSO-*d*₆) δ 2.5 (s, 3H, 6-CH₃), 3.7 (s, 3H, N-CH₃), 4.4 (m, 2H, NHCH₂Ph), 7.0–7.5 (m, 6H, Ar and 5-H (pyridinone)), 7.7–8.9 (br., OH), 9.3–9.8 (br., 1H, NH); MS (FAB): *m/z* 273 [(M-Cl)⁺]. Anal. calcd for C₁₅H₁₇ClN₂O₃: C, 58.35; H, 5.55; N, 9.07; Cl, 11.48%. Found: C, 58.57; H, 5.68; N, 8.98; Cl, 11.36%.

1,6-Dimethyl-3-hydroxypyridin-4(1H)-one-2-carboxy-(N-phenyl)-amide hydrochloride (15g). Yield 92%, mp 261–263 °C. ¹H NMR (methanol-*d*₄) δ 2.35 (s, 3H, 6-CH₃), 3.65 (s, 3H, N-CH₃), 6.8–7.6 (m, 6H, Ar and 5-H (pyridinone)); MS (FAB): *m/z* 348 [M⁺]. MS (FAB): *m/z* 259 [(M-Cl)⁺]. Anal. calcd for C₁₄H₁₅ClN₂O₃: C, 57.05; H, 5.13; N, 9.50; Cl, 12.03%. Found: C, 57.38; H, 5.26; N, 9.69; Cl, 11.96%.

1,6-Dimethyl-3-hydroxypyridin-4(1H)-one-2-carboxy-(N-3'-pyridyl)-amide dihydrochloride (15h). Yield 88%, mp 220 °C dec. ¹H NMR (D₂O) δ 2.4 (s, 3H, 6-CH₃), 3.6 (s, 3H, N-CH₃), 7.1 (s, 1H, 5-H(pyridinone)), 7.5–8.0 (m, 1H, 5-H(pyridine)), 8.1–8.6 (m, 2H, 4,6-H(pyridine)), 9.0 (s, 1H, 2-H(pyridine)); MS (FAB): *m/z* 260 [(M-HCl₂)⁺]. Anal. calcd for C₁₃H₁₅Cl₂N₃O₃: C, 47.00; H, 4.55; N, 12.65; Cl, 21.35%. Found: C, 47.27; H, 4.78; N, 12.89; Cl, 21.08%.

Determination of physicochemical properties of ligands

p*K*_a determination. Equilibrium constants of protonated ligands were determined using an automated computerized system, consisting of a Metrohm 665 dosimat, a Perkin-Elmer Lambda 5 UV/Vis Spectrophotometer, a Corning Delta 225 pH meter, and a 286 Opus PC which controlled the integrated system.^{8–10} A combined Sirius electrode (Sirius Analytical Instruments Ltd, Forest Row, East Sussex, UK) was used to calibrate the electrode zero and to measure pH values. This system is capable of undertaking simultaneous potentiometric and spectrophotometric measurements. A blank titration of 0.1 M KCl (25 mL) was carried out to determine the electrode zero using Gran's plot method.¹⁶ The solution (0.1 M KCl, 25 mL), contained in a jacketed titration cell, was acidified by 0.15 mL of 0.2 M HCl. Titration were carried out against 0.3 mL of 0.2 M KOH using 0.01 mL increments dispensed from the dosimat. Solutions were maintained at 25±0.5 °C under an argon atmosphere. The above titration was repeated in the presence of ligand. The data obtained from titration were subjected to non-linear least-square regression analysis using the NONLINM1 program.¹⁷ The p*K*_a values were obtained to an accuracy of ±0.02 pH unit.

Iron(III) stability constant determination. The cumulative iron(III) stability constants (β₃) for the ligands were determined by spectrophotometric competition titration of iron(III)–ligand complexes with EDTA using an automated system.¹⁰ The iron(III) complexes of the ligand were prepared in 10:1 molar ratio in 0.1 M 3-(*N*-morpholino)propanesulfonic acid (MOPS) buffer (pH 7.4). This solution was then titrated against EDTA (0.1 M in MOPS). The resulting spectrophotometric data were analysed using COMPT1 program and the cumulative stability constant were obtained to an accuracy of ±0.1 log unit.

The stepwise stability constants (*K*₁, *K*₂ and *K*₃) of the ligands were optimized from the spectrophotometric titration of the iron(III)–ligand.^{8–10} The analytical equipment used was similar to that used for p*K*_a determination. The electrodes were calibrated by titrating a volumetric standard strong acid with a volumetric standard strong base under argon gas. In order to maintain sufficient sensitivity, a 10 mm U.V. flow-cell was utilised. After electrode calibration, the solution was reacidified by adding concentrated hydrochloric acid and the pH of the solution was adjusted to 1.5–2.0. Iron(III) stock solution (atomic absorption standard, Aldrich) and the test ligand were then added to give a final ligand:iron(III) ratio of about 5:1. A preadjusted programmed

autoburette was used for the addition of a 0.2 M KOH solution. The resulting spectrophotometric titration curve was then subjected to non-linear least-square regression analysis.

Distribution coefficient determination. Distribution coefficients between 1-octanol and MOPS buffer (pH 7.4) were determined using an automated continuous flow technique.^{8–10} The aqueous and octanol phases were presaturated with respect to each other before use. The aqueous phase (50 mM MOPS buffer, pH 7.4) was separated from the two phase system (1-octanol/MOPS buffer, pH 7.4) by means of a hydrophilic cellulose filter 5 μm diameter, 589/3 Blauband filter paper, mounted in the gel-filtration column adjuster. A known volume (25–50 mL) of MOPS buffer (saturated with octanol) is taken in the flat base mixing chamber. After a base line was obtained, the solution was used for reference absorbance. The ligand to be examined was dissolved in buffer (saturated with octanol) so as to give an absorbance of between 0.5–1.5 absorbance units at the preselected wavelength (~280 nm). The 'online spectrophotometer' allows continuous assessment of the equilibrium of the aqueous phase. Once a stable UV absorbance is obtained, an aliquot of octanol is added and re-equilibration assessed. This cycle was repeated until a pre-defined total volume of added octanol is reached. The distribution coefficient (*D*_{7.4}) was calculated for each octanol addition using eq (4).

$$D_{7.4} = \frac{A_0 - A_1}{A_1} \times \frac{V_w}{V_o} \quad (4)$$

where *A*₀=initial absorbance of the aqueous phase; *A*₁=absorbance at equilibrium of aqueous phase after the addition of octanol; *V*_w=volume of the aqueous (MOPS buffer); and *V*_o=total volume of octanol after each addition.

Biological experiments

Male Wistar rats were purchased (local breed) from A. Tuck & Son (Battlesbridge, Essex SS1, UK) and housed in the Biological Service Unit, King's College London. The animals were maintained at a temperature between 20 and 23 °C, with food and water ad libitum. All animal experiments carried out have been specified in project licence PPL 70/4561 which was authorised by the Secretary of State (England) under Animals Act 1986.

Iron mobilisation efficacy study in ⁵⁹Fe-ferritin loaded rat. Hepatocytes of normal fasted rats (190–230 g) were labelled with ⁵⁹Fe by administration of ⁵⁹Fe-ferritin from tail vein.¹¹ One hour later, each rat was administered orally with chelator. Control rats were administered with an equivalent volume of water. The rats were placed in individual metabolic cages and urine and faeces collected. Rats were allowed access to food one hour after oral administration of chelator. There was no restriction of water throughout the study period. The investigation was terminated 24 h after the ⁵⁹Fe-ferritin administration, rats were sacrificed and the liver and

gastrointestinal tract (including its content and faeces) were removed for gamma counting. The “Iron mobilisation” and “Efficacy” were calculated according to following equations:

Iron mobilisation (%)

$$= \frac{{}^{59}\text{Fe-Activity}_{(\text{Gut \& Faeces})}}{{}^{59}\text{Fe-Activity}_{(\text{Gut \& Faeces})} + {}^{59}\text{Fe-Activity}_{(\text{Liver})}} \times 100\% \quad (5)$$

Efficacy (%) = Iron mobilisation (%)

$$- \text{control} (\%) \quad (6)$$

In vivo metabolism study using rat bile cannulation model.

Normal fasted Wistar rats weighing approximately 250–300 g were anaesthetised by combined ip application of Hypnorm[®] (a mixture of fentanyl citrate and fluanisone) and Hypnovel[®] (midazolam). The cannulation of bile duct was undertaken followed by exteriorisation of cannulae. Chelators (450 µmol/kg body weight) were administered orally by gavage. Bile samples were collected at hourly intervals to 10 h. The urine and faeces samples were also simultaneously collected while the animal was placed in a metabolism cage. At the completion of bile collection, the gastrointestinal tract (GIT) including the contents were collected, chopped to small pieces, stirred in water and filtered. The volume of the filtrate was adjusted to 100 mL using water in order to calculate the amount of unabsorbed chelator.

Sample analysis. The bile, urine and GIT samples were filtered using the syringe filters (13 mm GD/X disposable filter device, 0.2 µm pore size). The filtrates were injected into HPLC for analysis. A Hewlett Packard Model 1090M Series-II HPLC system complete with an auto injector, auto sampler and diode array detector, linked to a HP 900–300 data station was used in the present study. A polymer PLRP-S column (15×0.46 cm) and a gradient ion-pair mobile phase system,¹⁸ utilising water (containing 5 mM sodium 1-heptanesulfonate) and acetonitrile, were used for the separation of the analytes and mobile phase. The eluents were monitored at 280 nm.

In order to determine the glucuronidation metabolite, bile and urine samples were incubated in the absence (controls) or presence of β-glucuronidase in 60 mM MOPS buffer, pH 7.4 (the final concentration of 2000 units/mL) for 16 h at 37 °C. After filtration, the unchanged chelators were determined as above and the difference between the control and the β-glucuronidase

treated sample was accounted as the amount of glucuronidated metabolite.

Acknowledgements

The authors would like to thank Apotex Research Inc. Canada and Biomed EC grant BMH4-CT97-2149 for supporting this research project.

References and Notes

1. Brittenham, G. M. In: *Hematology: Basic Principles and Practice*. Hoffman, R., Benz, E., Shattil, S., Furie, B., Cohen, H., Eds.; Churchill Livingstone: New York, 1991; pp 327–349.
2. Hershko, C.; Konijn, A. M.; Link, G. *Br. J. Haematol.* **1998**, *101*, 399.
3. Tilbrook, G. S.; Hider, R. C. In *Metal Ions in Biological Systems. Vol. 35: Iron Transport and Storage in Microorganisms, Plants and Animals*, Sigel, A., Sigel, H., Eds.; Marcel Dekker: New York, 1998; pp 691–730.
4. Hider, R. C.; Khodr, H.; Liu, Z. D.; Tilbrook, G. In *Metal Ions in Biology and Medicine*, Collery, Ph., Brätter, P., Negretti, de Brätter V., Khassanova L., Etienne J. C., Eds. John Libbey Eurotext: Paris, 1998, Vol. 5, pp 51–55.
5. Zbinden P. *Hydroxypyridinones*. US Patent 5,688,815, 1997.
6. Hider, R. C.; Tilbrook, G. S.; Liu, Z. D. International Patent WO 98/54138, 1998.
7. Lowther, N.; Fox, P.; Faller, B.; Nick, H.; Jin, Y.; Sergejew, T.; Hirschberg, Y.; Oberle, R.; Donnelly, H. *Pharmaceut. Res.* **1999**, *16*, 434.
8. Liu, Z. D.; Khodr, H. H.; Liu, D. Y.; Lu, S. L.; Hider, R. C. *J. Med. Chem.* **1999**, *42*, 4814.
9. Dobbin, P. S.; Hider, R. C.; Hall, A. D.; Taylor, P. D.; Sarpong, P.; Porter, J. B.; Xiao, G.; van der Helm, D. *J. Med. Chem.* **1993**, *36*, 2448.
10. Rai, B. L.; Dekhordi, L. S.; Khodr, H.; Jin, Y.; Liu, Z. D.; Hider, R. C. *J. Med. Chem.* **1998**, *41*, 3347.
11. Liu, Z. D.; Lu, S. L.; Hider, R. C. *Biochem. Pharmacol.* **1999**, *57*, 559.
12. Xu, J. D.; Kullgren, B.; Durbin, P. W.; Raymond, K. N. *J. Med. Chem.* **1995**, *38*, 2606.
13. Pippard, M. J.; Johnson, D. K.; Finch, C. A. *Blood* **1981**, *58*, 685.
14. Singh, S.; Choudhury, R.; Epemolu, R. O.; Hider, R. C. *Eur. J. Drug Metab. Pharmacokinet* **1996**, *21*, 33.
15. Ellis, B. L.; Duhme, A. K.; Hider, R. C.; Hossain, M. B.; Rizvi, S.; van der Helm, D. *J. Med. Chem.* **1996**, *39*, 3659.
16. Gran, G. *Analyst* **1952**, *77*, 661.
17. Taylor, P. D.; Morrison, I. E. G.; Hider, R. C. *Talanta* **1988**, *35*, 507.
18. Liu, D. Y.; Liu, Z. D.; Lu, S. L.; Hider, R. C. *J. Chromatogr. B* **1999**, *730*, 135.